

Radionuclide Bone Scanning in Giant Cell Tumor

Douglas Van Nostrand, John E. Madewell, Lawrence M. McNiesh, Ralph W. Kyle,
and Donald Sweet

*Walter Reed Army Medical Center; Armed Forces Institute of Pathology; and Uniformed Services
University of Health Sciences, Washington, DC*

Radionuclide bone scan findings are described and correlated with pathology in 23 patients with giant cell tumor (GCT) of the bone. The degree of radionuclide activity was markedly increased in 20 (87%), minimally increased in three (13%), and decreased in none of the patients. Of the 23 patients with increased radioactivity, the pattern was diffuse in 11 (48%) and doughnut in 12 (52%). Extended patterns of radioactivity were present in 19 of 22 patients; however, none were associated with true tumor extension. Bone scanning did not aid in the detection of GCT, was nonspecific, and did not differentiate benign from malignant GCT. Although radioactivity extended beyond the radiographic abnormality in the majority of patients, this was most likely secondary to other bony abnormalities or local and/or regional hyperemia, and caution should be taken in ascribing this extension to either tumor or metastasis.

J Nucl Med 27:329-338, 1986

Radionuclide bone scanning has been used in the evaluation of bone neoplasms as a possible aid in (a) detection, (b) differential diagnosis, (c) differentiating benign from malignant lesions, (d) defining local extent of tumor, and/or (e) demonstrating distant skeletal involvement (1,2). Accordingly, it is important to characterize the radionuclide bone scan appearance, to correlate these findings with pathology, and to determine the clinical role of bone scanning for each bone neoplasm. Bone scan findings in giant cell tumor (GCT) have been previously reported (3,4). The purpose of this report is to confirm and further describe the appearance of GCT on radionuclide bone scanning, to visually correlate these findings with the histopathology, to review the literature, and to help determine the role of radionuclide bone scanning in the evaluation of GCT.

MATERIALS AND METHODS

A retrospective review of 23 patients (five at Walter Reed Army Medical Center and 18 patients at the Armed Forces Institute of Pathology) with pathologically proven GCT was undertaken. No patient with

aneurysmal bone cyst was included. The following were reviewed: (a) clinical summary, (b) preoperative radiographs of the lesion, and (c) preoperative radionuclide bone imaging of the lesion.

Clinical summaries were reviewed for age, sex, presenting signs and symptoms, and history of trauma.

Radiographs performed with standard techniques were interpreted by two of the authors (J.M. and L.M.). The location of the lesion was noted and categorized according to a previously described classification in the literature (5). The radiologic pattern was described as either 1a, 1b, 1c, II, or III and defined as follows: 1a: Geographic destruction, well-defined with sclerosis in margin; 1b: geographic destruction, well-defined but no sclerosis in margin; 1c: geographic destruction with ill-defined margin; II: moth-eaten; and III: permeated. Additional radiographic features such as expansion, periosteal reaction, and soft-tissue swelling were noted if present.

Bone scans were performed preoperatively with technetium-99m (^{99m}Tc) phosphate radiopharmaceuticals in all patients. Images were obtained at standard times with a gamma camera in 22 patients and a rectilinear scanner in one patient. Abnormalities on bone scans were evaluated for intensity, pattern, and extended patterns (6) defined as follows:

Intensity of abnormality on bone scan. Hot: marked increased radioactivity relative to adjacent or contralateral bone (Figs. 3B,4B,5B); warm: slight but definite

Received May 21, 1985; revision accepted Nov. 11, 1985.

For reprints contact: Douglas Van Nostrand, MD, HSHL-XN, Chief, Nuclear Medicine Service, Walter Reed Army Medical Center, Washington, DC 20307-5001.

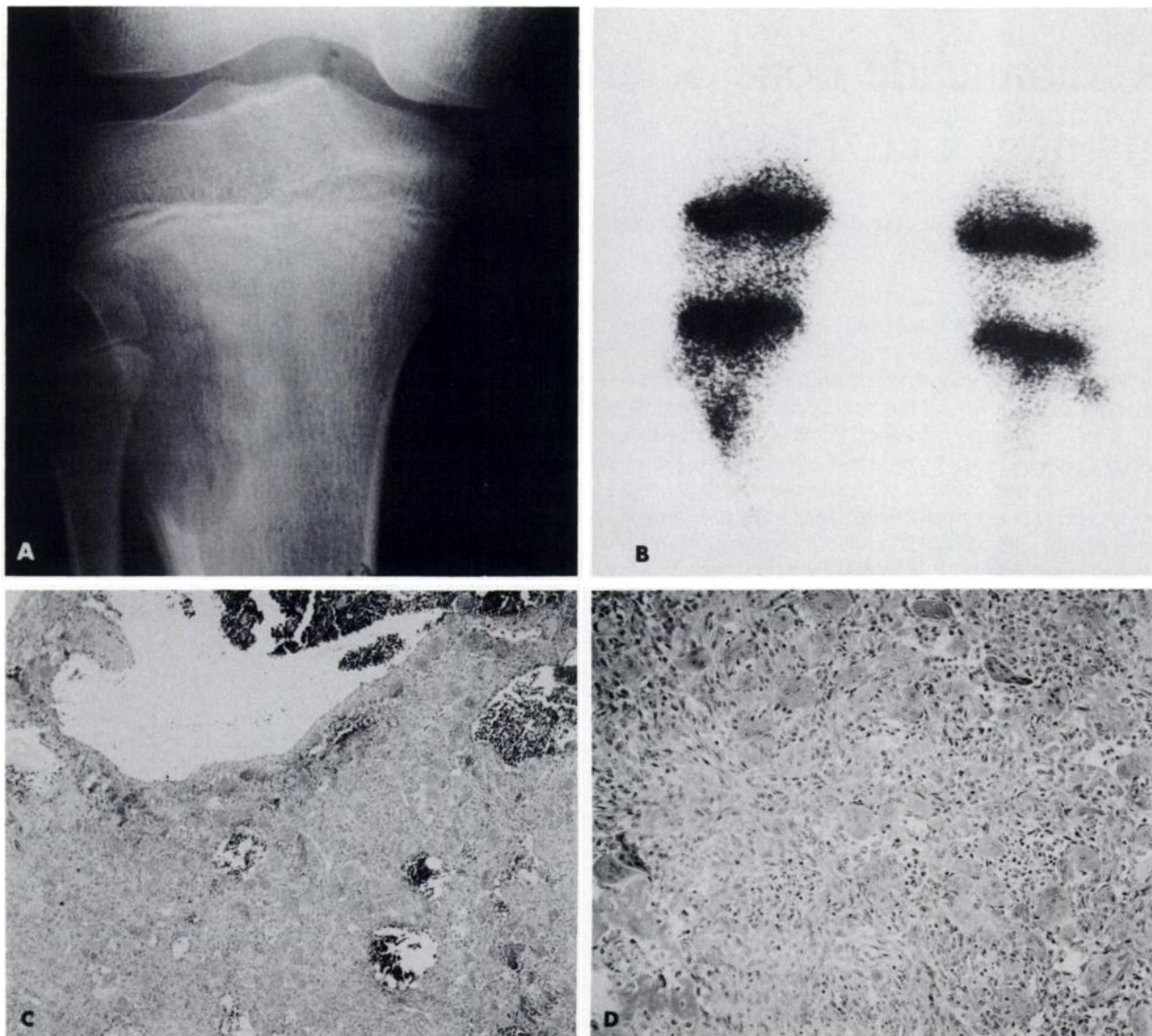


FIGURE 1

Case 4. A: AP radiograph shows 1b lytic lesion in metaphysis of proximal tibia with eccentric location and layered codman angle periosteal reaction. B: Anterior bone scan demonstrates "warm" uptake of radioactivity corresponding to radiographic abnormality. Radioactivity around periphery is irregular, and center has relatively less radioactivity than periphery. Increased radioactivity is present contiguous and noncontiguous to bony abnormality on radiograph. C: 63 X H&E photomicrograph demonstrates GCT with area of cyst formation and several dilated vascular channels. (AFIP Neg No. 84-12802-2). D: 160 X H&E photomicrograph demonstrates numerous multinucleated osteoclastic giant cells in slightly fibrous to oval stromal background. Osteoid elaboration (arrow) is present adjacent to reactive margin.

increased activity relative to adjacent or contralateral bone (Figs. 1B,2B); cold: decreased activity relative to adjacent or contralateral bone; and normal.

Pattern of bone scan abnormality. Diffuse (solid) (Fig. 2B); and doughnut (Figs. 1B,4B,5B).

Extended pattern (Figs. 1B,4B,5B). Abnormal radioactivity that is present beyond the radiographic abnormality and is either contiguous and/or noncontiguous (distant to) to the radiographic abnormality. If a radiographic abnormality was present that could explain the extended pattern (i.e. degenerative joint dis-

ease), then this area was excluded from analysis. Whole-body scans were not available for review in all cases. In such instances, the bone scan report or narrative summary was used to determine the presence or absence of skeletal metastasis.

RESULTS

Twenty-three patients were reviewed. The age, presenting signs and symptoms, radiographic classification, bone scan findings, and pathology for the 18 benign GCTs are noted in Table 1 and for the five

TABLE 1
Benign Giant Cell Tumor

Case No.	Age/ Sex	Presenting symptom	Bone	Radiograph	Bone scan	CEF [†]	NCEF [‡]	Histology
1	24/F	Pain	Proximal middle phalanx	1b Expansile soft tissue swelling	Hot, Diffuse	+ [§]	+	GCT
2	39/M	Low back pain lifting wood	Pedicles of T-12	1b Lysis of pedicles and posterior vertebral body of T-12 Soft tissue mass	Warm, Diffuse	ID**	ID	GCT with partial cystic change
3	38/M	Persistent knee pain after minor trauma	Distal femur	1c	Hot, Diffuse	+	+	GCT with secondary cyst formation
4*	10/F	Thigh pain	Proximal tibia	1b	Warm, Doughnut	+	+	GCT with secondary cyst formation and reactive bone
5	50/F	Pain and swelling	Proximal phalanx, 4th	II	Hot, Diffuse	+	- [†]	GCT
6	19/M	Shoulder pain after moving furniture	Acromium/scapula	II Expansile	Hot, Diffuse	+	+	GCT with secondary cyst formation
7*	17/F	Pain in back	Pedicle and body of T-10	No grade expansile, lysis of pedicle and body of T-10	Warm, Diffuse	-	-	GCT with secondary reactive osteoblastic activity
8	27/M	Pain for 13 months	Proximal tibia	1a-b	Hot, Diffuse	+	+	GCT with loose stroma fibrin
9	33/M	Pain moving furniture	Proximal tibia	1b	Hot, Diffuse	-	-	GCT with secondary cyst formation and reactive bone
10	20/F	Mass	Medial clavicle	1c Soft tissue mass, expansile	Hot, Doughnut	-	-	GCT with telangiectasia and osseous shell
11	24/F	Pain	Distal femur	1b	Hot, Diffuse	+	+	GCT with recurrence
12*	20/M	Pain for 5 months with swelling	Proximal tibia	1b	Hot, Doughnut (Ring)	+	+	GCT
13	30/M	Mass	Metatarsal	1b	Hot, Diffuse	+	+	GCT
14	22/F	Pain and mass	Distal radius	1b Expansile	Hot, Doughnut	+	+	GCT with spindle stroma
15	28/M	Pain for one month	Proximal humerus	1c	Hot, Doughnut	-	+	GCT with increased vascularity
16	42/F	Pain 1 year after fall	Proximal fibula	1c Expansile	Hot, Doughnut	-	+	GCT with increased cellular activity and reactive margin
17	23/F	Pain and swelling for ten months	Distal femur	1c Expansile soft tissue mass	Hot, Doughnut	+	+	GCT with central necrosis
18*	25/M	Pain	Proximal radius	1c Lytic Expansile	Hot, Doughnut	-	+	GCT with reactive margin

* See figures. † CEF = Contiguous extended field (see text). ‡ NCEF = Noncontiguous extended field (see text).

§ Present. † Absent. ** Indeterminate.

TABLE 2
Malignant Cell Tumors

Case No.	Age/ Sex	Presenting symptom	Bone	Radiograph	Bone scan	CEF [†]	NCEF [‡]	Histology
19*	74/F	Pain	Ilium	1c	Hot, Doughnut	+ [§]	+	Malignant GCT with partial necrosis and hemorrhage
20*	62/F	Weakness in thumb	Distal radius	1c Expansile	Hot, Doughnut	+	+	Malignant GCT
21	29/F	Pain and limited range of motion	Proximal tibia	1b	Hot, Diffuse	+	+	Malignant GCT
22	19/M	Intermittent pain and swelling	Proximal tibia	1a	Hot, Doughnut	+	+	GCT with early malignant stromal change
23	55/M	Pain	Distal femur	1c Expansile	Hot, Doughnut	+	+	GCT with early malignant stromal change

* See figures.

† CEF = Contiguous extended field (see text).

‡ NCEF = Noncontiguous extended field (see text).

§ Present.

malignant GCTs in Table 2. Twelve patients were females and 11 were males with a median age of 31.7 yr.

Of the 23 patients, 20 (87%) had marked increased activity (hot), three (13%) had slight but definite increased activity (warm), and none had decreased activity (cold). The bone scan pattern in those cases with increased activity was diffuse (solid) in 11 (48%), and doughnut in 12 (52%). The latter appeared with varying widths of radioactive uptake from a thin ring to a thick doughnut. An extended pattern of radioactivity was present in 19/22 patients. In 16 patients, the extended pattern was contiguous to the radiographic abnormality, and in 18 patients the extended pattern was noncontiguous to the radiographic abnormality. Fifteen patients had both contiguous and noncontiguous extension. One patient was indeterminate. No skeletal metastases or additional GCTs were detected on preoperative bone scan.

DISCUSSION

Clinical

Giant cell tumor usually has an insidious onset and may become large before signs or symptoms develop. Often the patient presents with persistent pain following trauma with occasional mass or swelling. Because the tumor is often large, range of motion in the adjacent joint may be limited.

Pathologic

The origin of GCT is controversial, but the tumor most likely arises from osteoclasts and is typically

formed of multinucleated giant cells within a background of intervening stromal cells. There is often a striking sinusoidal vascular bed with focal telangiectasia. Involutional changes such as fibrosis, necrosis, and cyst formation are seen with some frequency. Osteoblastic activity is usually confined to the peripheral reactive margin (9,10).

Radiologic

The characteristic radiographic appearance is an "expansile" radiolucent lesion in the metaepiphyseal end of long bones usually extending to the subarticular bony plate. In patients with open growth plates, GCT may arise in the metaphysis adjacent to the epiphyseal growth plate. GCT rarely involves the joint space directly, but not infrequently a joint effusion may be present. Generally, no significant new bone formation other than the expanded periosteal shell or endosteal reaction is noted. GCTs are usually geographic lesions with margins ranging from well-defined (1b) to ill-defined (1c). These tumors often disrupt the cortex, and pathologic fracture may be noted. The radiographs do not reliably distinguish benign from malignant GCT (7,8).

Radionuclide Findings

Numerous authors have reported radionuclide bone scan findings in GCT (3,4,11-15); a review of three series are shown in Tables 3 and 4. The degree of radioactivity in GCT was hot in 94% (76/81), warm in

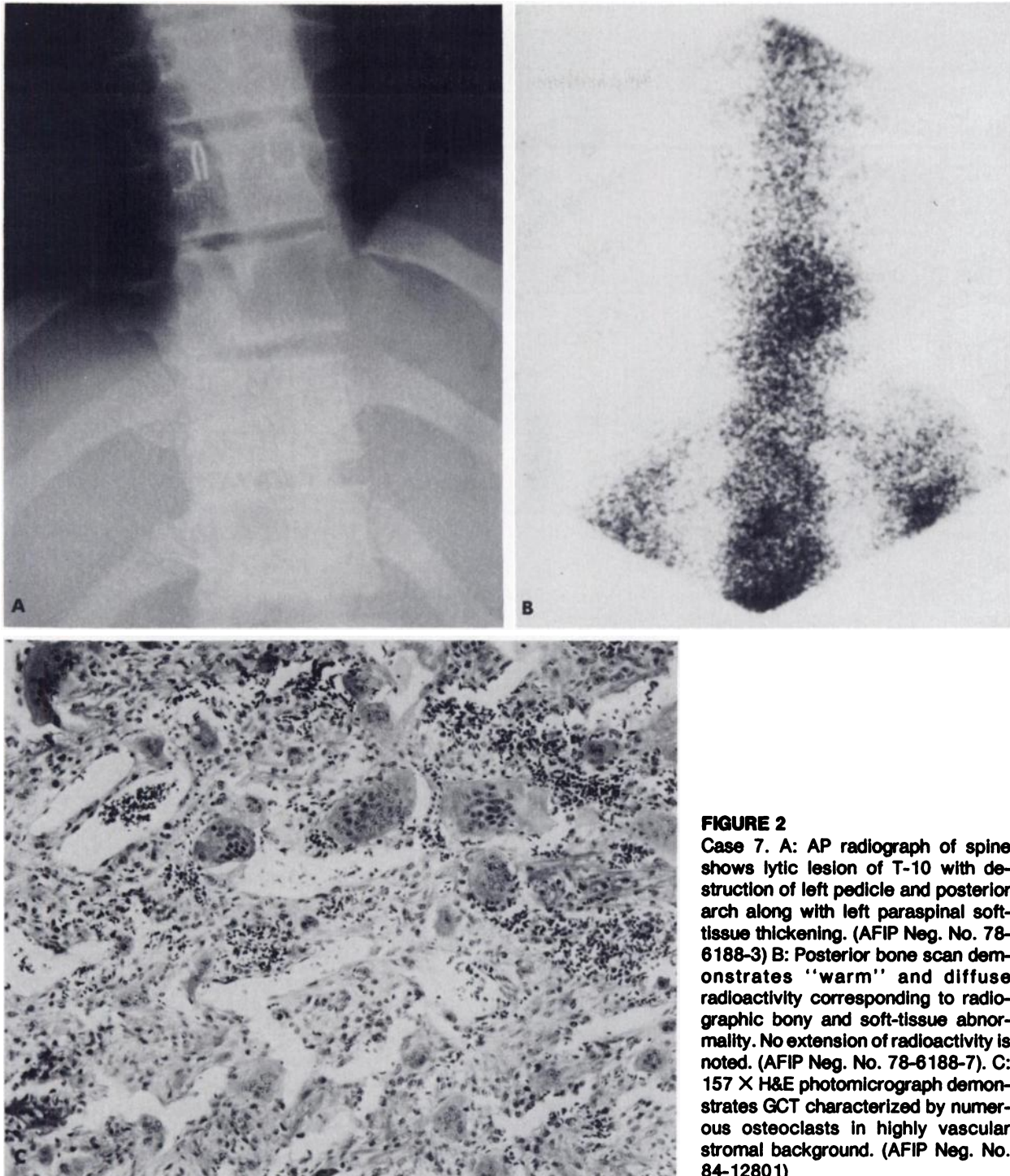


FIGURE 2

Case 7. A: AP radiograph of spine shows lytic lesion of T-10 with destruction of left pedicle and posterior arch along with left paraspinal soft-tissue thickening. (AFIP Neg. No. 78-6188-3) B: Posterior bone scan demonstrates "warm" and diffuse radioactivity corresponding to radiographic bony and soft-tissue abnormality. No extension of radioactivity is noted. (AFIP Neg. No. 78-6188-7). C: 157 X H&E photomicrograph demonstrates GCT characterized by numerous osteoclasts in highly vascular stromal background. (AFIP Neg. No. 84-12801)

6% (5/81), and normal or cold in none. GCT had a diffuse pattern of radioactive uptake in 40% (32/81) and a doughnut pattern in 60% (49/81). One patient (1%) had a "skip" lesion, and one patient (1%) had a second foci of GCT. Except for this report, patients were not subdivided into malignant or benign GCT; no metastasis were noted on bone scan. The extent of tumor was similar or identical to the extent of radioactivity on bone scan in 31% (25/81) as determined by

radiographs, tomography, and/or histopathology. Bone scan underestimated the extent of tumor in one of 81 patients (1%). Contiguous and noncontiguous extension were noted in 54% (44/81) and 67% (54/81), respectively. Hudson (3) reported one patient who had a second GCT that was masked by the extended radioactivity from another GCT, and Levine (4) noted the bone scan did not demonstrate soft-tissue extension of tumor in nine patients.

TABLE 3
Collected Series
(Radionuclide Bone Scan Findings in GCT)

Author	Ref	Total	Hot	Warm	Normal or cold	Diffuse	Doughnut
Hudson	3	37	37	0	0	12	25
Levine	4	21	19	2	0	9	12
Van Nostrand	—	23	20	3	0	11	12
		81	76 (94%)	5 (6%)	0	32 (40%)	49 (60%)

TABLE 4
Collected Series
(Radionuclide Bone Scan Findings in GCT)

Author	Ref	Total	"Skip" Lesions	Multifocal GCT	Meta-stasis	Extension				ID [†]
						Smaller	Identical	Larger		
							Contiguous	Noncontiguous		
Hudson	3	37	0	1	0	0	12	18	23	0
Levine	4	21	1	0	0	1	10	10	13*	0
Van Nostrand	—	23	0	0	0	0	3	16	18	1
		81	1(1%)	1(1%)	0	1(1%)	25(31%)	44(54%)	54(67%)	1(1%)

* Five patients had joint invasion.

† Indeterminate.

Mechanism of Radioactive Uptake

The mechanism for increased radioactive uptake has been ascribed to increased blood flow and reactive bone formation around the periphery of the lesion (16). Although increased blood flow in GCT has been well documented by angiography (17-19), Levine (4) was unable to demonstrate any relationship between degree of radioactivity uptake and vascularity in eight patients. Increased reactive bone formation results from both endosteal (Case 20, Fig. 6) and periosteal reaction (Case 18, Fig. 4D) attempting to contain the expansile mass, and the reactive bone formation appears to be a major mechanism for increased radioactivity.

Mechanism of Radioactive Pattern

The variation in observed bone scan patterns (diffuse and doughnut) may be due to one or a combination of factors such as (a) degree/width of the reactive bone margin, (b) imaging technique, and/or (c) size of lesion. As noted previously, the tumor is formed of multinucleated giant cells and interspersed stromal cells. Little or no osteoblastic activity with bone formation is typically encountered centrally in most GCTs (Case 18, Fig. 4C and Case 19, Fig. 5C). Furthermore, secondary telangiectasia (Case 4, Fig. 1C), cyst formation (Case 4, Fig. 1C), and occasionally necrosis (Case 19, Fig. 5D)

is seen within the midst of many GCTs. Accordingly, significant radiolabeled phosphate activity would not be anticipated centrally relative to the expected and demonstrated radionuclide activity in a spherical encompassing bony shell (Case 18, Fig. 4D) around the tumor. When a three-dimensional spherical shell is viewed in two dimensions, the central aspect will have less radioactivity relative to the circumference which gives the appearance of a doughnut. The ability of the imaging system to demonstrate a doughnut rather than a diffuse pattern may be compromised by the width of reactive bone margin around the periphery, improper technique (i.e., intensity of camera too high), or size. With improved techniques, more lesions may be demonstrated as a doughnut rather than a diffuse pattern (Case 18, Fig. 4B).

Mechanism and Utility of Contiguous Uptake

The mechanism for increased radioactivity extending beyond, but contiguous to, the radiographic abnormality has been previously discussed and attributed to increased blood flow (4,6). Although some extension of radioactivity could have been secondary to actual tumor extension beyond the radiographically defineable limits or poor imaging technique with high camera intensities ("blossoming"), this mechanism could not

account for all the cases with extended radioactivity. Because of the above-described contiguous extended radioactivity, one may not reliably use the bone scan to accurately define the extent of tumor; however, with one exception in the three series, the bone scan reliably defined maximal limit of extent. Nevertheless, other imaging modalities such as plain radiographs, conventional tomography, computed tomography, and magnetic resonance better define tumor extent (3,4).

Mechanism and Utility of Noncontiguous Uptake

The mechanism for noncontiguous extension of radioactivity (with no bone abnormality) remains incompletely understood; however, it may reflect some degree of increased bone turnover secondary to active hyperemia mediated through a neurocirculatory reflex mechanism (20,21). This may also account for a noncontiguous extended pattern when a contiguous pattern was not present (Case 7, Fig. 2B, and Cases 9, and 10). Although noncontiguous extension is often less intense than the area of primary tumor, one cannot distinguish between benign and malignant extension.

Sensitivity and Specificity

In the literature and this study, no GCT was detected on bone scan that was not easily seen on plain radiographs. Although specificity was not addressed in these series, the diffuse pattern on bone scan is not specific for GCT as many other benign (2,22) and malignant neoplasms (23,24) may demonstrate a similar appearance. The doughnut pattern has also been reported in other bone lesions such as simple bone cyst and eosinophilic granuloma (1). The thin-rimmed doughnut pattern is also typical for most benign and malignant neoplasms and has been reported in "aneurysmal bone cyst" (25) and bone infarction (26,27). In this report, no bone pattern or degree of intensity of radioactivity was identified which aided in the differentiation of benign from malignant GCT.

Detection of Multicentric GCT

Multicentric foci of GCT have been reported in 0.4% of patients (28) and in as high as 18% of patients with GCT of the hand (28). As noted earlier, only one of 81 patients had a multicentric foci of GCT. Although Averill (28) has suggested the use of bone scan to demonstrate these multicentric foci in patients with GCT of the hand, this awaits further confirmation.

Detection of Other Bony Diseases

Bone scan may potentially alter the differential diagnosis of a radiographic abnormality by demonstrating multiple focal bony abnormalities elsewhere such as in histiocytosis X, fibrous dysplasia, enchondroma, or diffuse bony metastasis (29). Since all the series in this review were retrospective, the value of preoperative

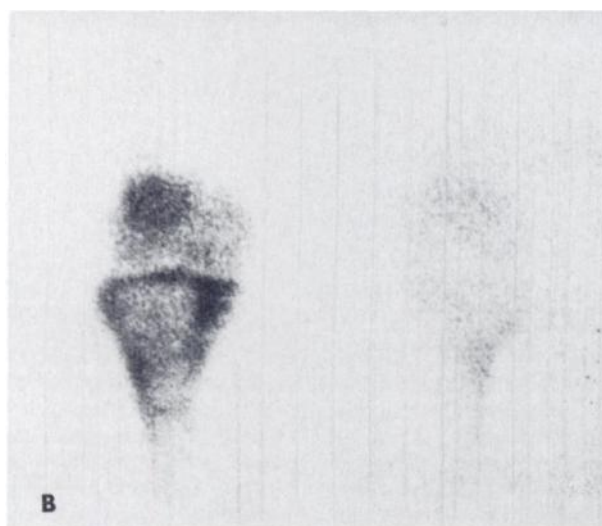


FIGURE 3

Case 12. A: AP radiograph shows diffuse osteoporosis about knee with large lytic lesion in proximal tibia extending to subarticular plate. B: Anterior bone scan demonstrates increased radioactivity in area corresponding to radiographic abnormality. Radioactivity is most marked (hot) around the periphery, which gives appearance of ring. When comparing both knees, increased radioactivity is noted contiguous and noncontiguous (femur) to radiographic abnormality

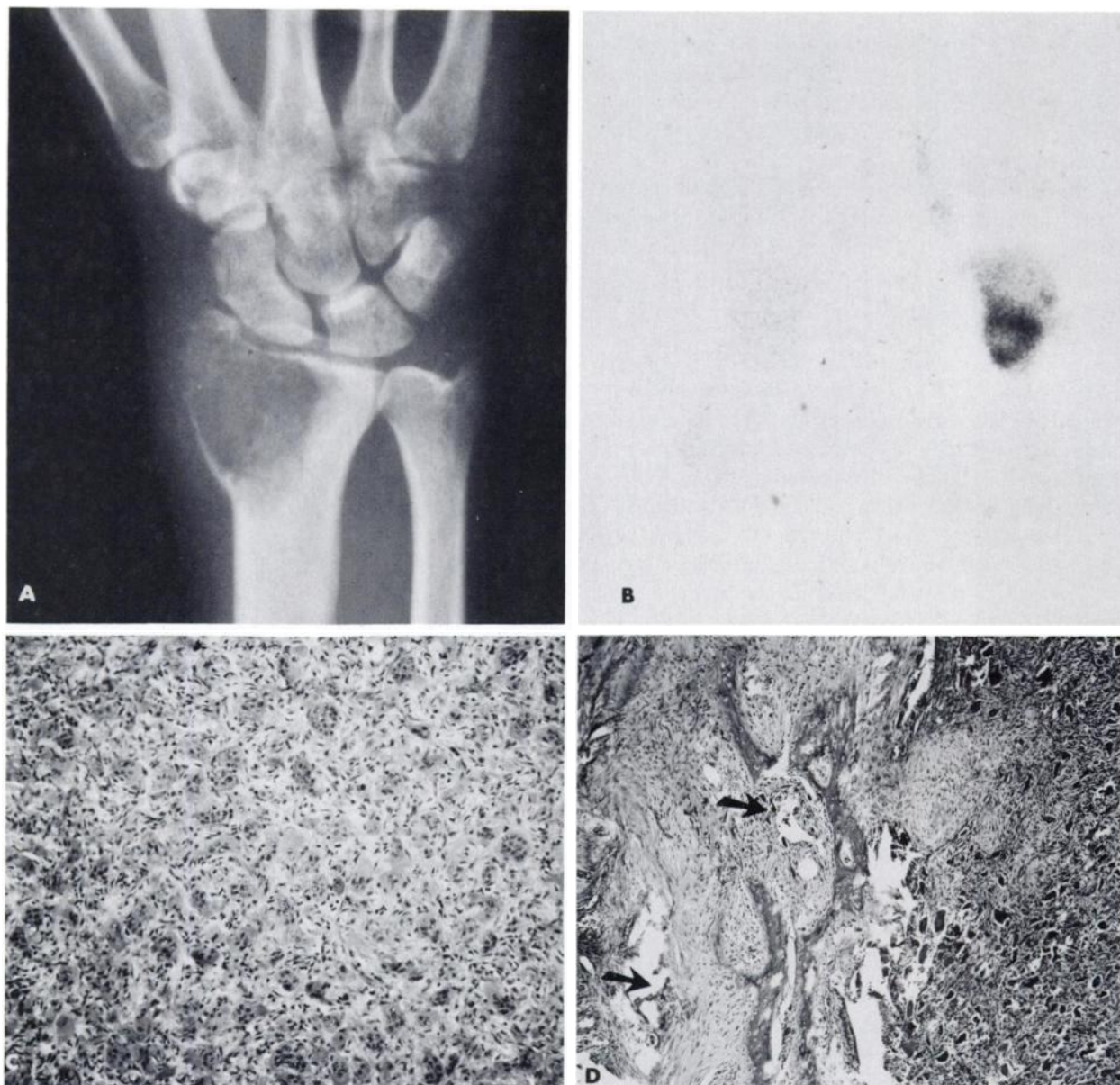


FIGURE 4

Case 18. A: Radiograph of wrist demonstrates expansile predominantly 1c lytic lesion with some moth-eaten character to margin. Adjacent soft-tissue swelling with patchy osteoporosis of carpal bones is seen. B: Palmar view on bone scan demonstrates increased (hot) radioactivity in doughnut pattern confined to radiographic abnormality; however, doughnut has slightly less radioactivity on radial side. Noncontiguous extension of radioactivity is noted in first phalanx and carpal bones. C: 160 X H&E photomicrograph demonstrates GCT with tightly packed osteoclasts in slightly spindled background. D: 60 X H&E photomicrograph demonstrates GCT escaping confines of its reactive bony periosteal shell (arrows).

bone scan in this area cannot be assessed; in addition, its value will depend on the prevalence of the various diseases in the referred patient population.

SUMMARY

In summary, this paper describes the bone scan findings in giant cell tumor in 23 patients and reviews the literature. Typically, GCT has marked increased radio-

activity; sometimes, however, radioactivity is only minimally increased. The pattern is typically diffuse or doughnut in configuration, and the major mechanism for increased radioactivity appears to be reactive bone formation while blood flow may play a more minor role. The doughnut pattern appears to be secondary to (a) increased peripheral radioactivity secondary to reactive bone formation, (b) relative absences of radioactivity in the center secondary to histopathology (giant cells,

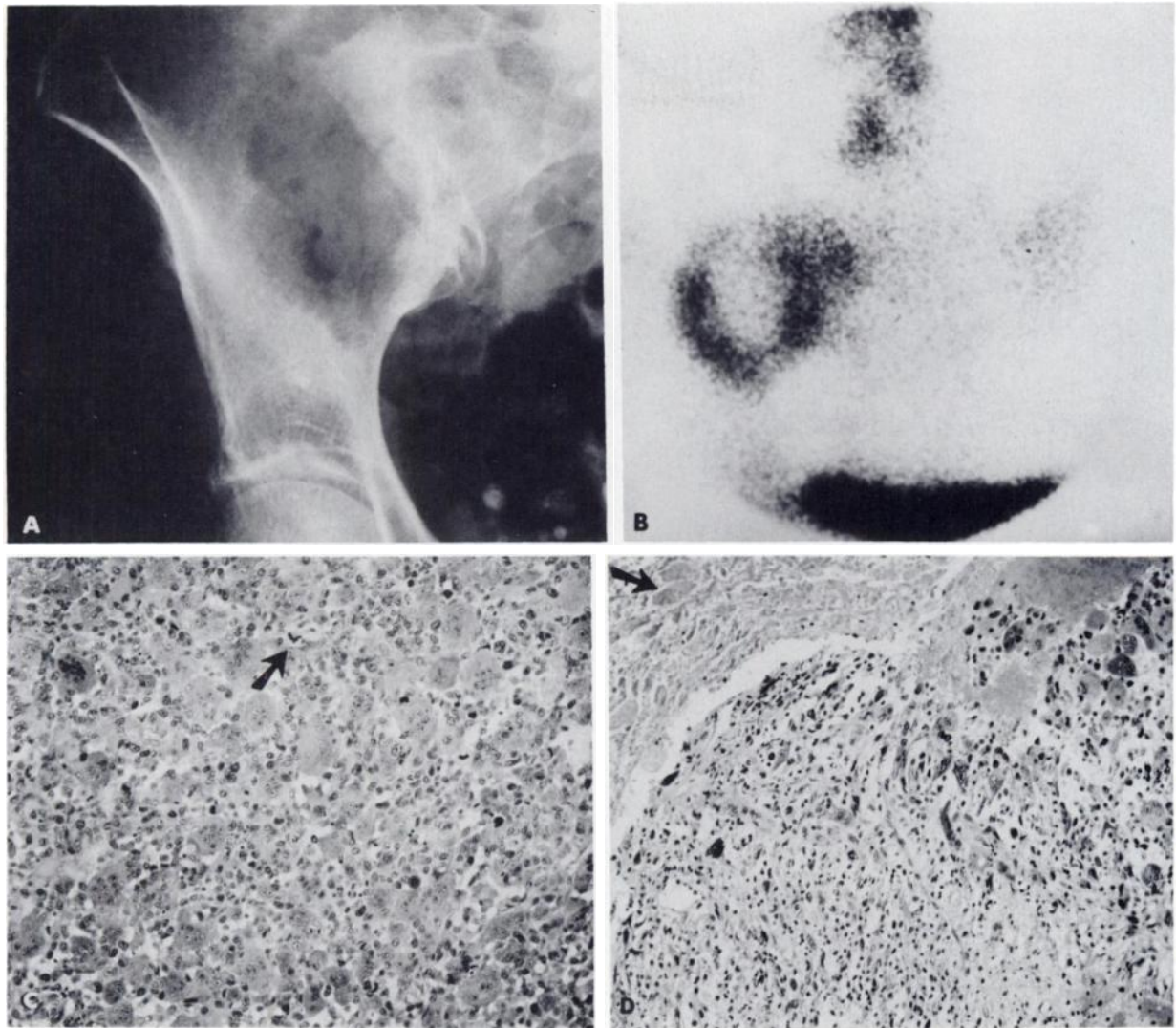


FIGURE 5

Case 19. A: AP radiograph of pelvis demonstrates 1c lytic lesion in ilium. B: Anterior bone scan of pelvis demonstrates increased (hot) radioactivity with doughnut pattern corresponding to radiographic abnormality. Contiguous and noncontiguous extension (sacroiliac joint) is noted. C: 157 X H&E photomicrograph demonstrates GCT with moderately hyperchromatic, pleomorphic, and mitotically active stromal background. Note atypical mitosis (arrow). D: 157 X H&E photomicrograph demonstrates margin between necrotic GCT (arrow) and moderately pleomorphic viable tumor.

necrosis, cysts, telangiectasias), and (c) camera resolution and technique. With improved imaging technique, the doughnut pattern may be seen more frequently.

Preoperative bone scan detected no GCT that was not demonstrated radiographically, and no pattern of radioactivity in the area of the radiographic abnormality aided in the differential diagnosis or differentiation of benign from malignant GCT. Contiguous and noncontiguous extended patterns of radioactivity routinely occurred and may be secondary to hyperemia and/or a neurocirculatory reflex mechanism. Because of these extended patterns, bone scan cannot accurately predict the true extent of the tumor in bone or soft tissue. Other diagnostic modalities are clearly superior. Bone scanning can aid in the demonstration of "skip" lesions,

multifocal GCT, or metastasis; however, these appear to be infrequent.

ACKNOWLEDGMENTS

The authors thank Ms. Mary Sue Mood and Ms. Lorraine Woodruff for assistance in the preparation of this manuscript.

The opinion and assertions contained herein are the private views of the author and are not to be construed as official or as reflecting the views of the Department of the Army or the Department of the Defense.

REFERENCES

1. Gilday DC, Ash JM: Benign bone tumors. *Semin Nucl Med* 6:33-46, 1976



FIGURE 6

Case 20. 60 X H&E photomicrograph from resected distal radius demonstrates reactive endosteal bone formation about margin of GCT. At this low power, tumor's malignant features are not obvious.

2. Kirchner PT: *Nuclear Medicine Review Syllabus*, New York, The Society of Nuclear Medicine, 1980, pp 559-562
3. Hudson TM, Schiebler M, Springfield DS, et al: Radiology of giant cell tumors of bone: Computer tomography, arthrotomography and scintigraphy. *Skel Radiol* 11:85-95, 1984
4. Levine E, DeSmet AA, Neff JR, et al: Scintigraphy evaluation of giant cell tumor of bone. *Am J Roentgenol* 143:343-348, 1984
5. Madwell JE, Ragsdale BD, Sweet DE: Radiologic and pathologic analysis of solitary bone lesions. *Radiol Clin North Am* 19:715-748, 1981
6. Thrall JH, Geslien GE, Corcoran RJ, et al: Abnormal radionuclide deposition patterns adjacent to focal skeletal lesions. *Radiology* 115:649-633, 1975
7. Spranger JW, Langer LO, Wiedemann HR: *Bone Dysplasias: An Atlas of Constitutional Disorders of Skeletal Development*, Philadelphia, Saunders, 1974, pp 81
8. Edeiken J, Hodes PJ: *Roentgen Diagnosis of Disease of Bone*, Baltimore, Williams & Wilkins, 1973, pp 998-1005
9. Jaffee HL: Histogenesis of bone tumors, tumors of bone and soft tissue. *8th Annual Clinical Conference at the University of Texas, M.D. Anderson Hospital*, 1963, pp 47
10. Jaffee HL: *Tumors and Tumorlike Conditions of the Bones and Joints*, Philadelphia, Lea & Febiger, 1958, pp 18-43
11. Moon NF: The clinical use of sodium fluoride F-18 in bone photoscanning. *JAMA* 204:974, 1968
12. Sneppen O, Heerfordt J, Dissing I, et al: Numerical assessment of bone scintigraphy in primary bone tumors and tumor-like conditions. *J Bone Joint Surg* 60:966-969, 1978
13. Toffe N, Littleton MA: *Scintigraphy in Pediatric Bone Tumors. Bone Tumors in Children, Vol II*, PSG Publishing Co, 1979, pp 79-90
14. Fordham EW, Ali A, Turner DA, et al: *Atlas of Total Body Radionuclide Imaging, Vol 1*, Philadelphia, Harper & Row, 1972
15. McLean RG, Murray IPC: Three-phase skeletal scintigraphy for suspected bone tumors. *Clin Nucl Med* 9:378-382, 1984
16. Charkes ND: Mechanisms of skeletal tracer uptake. *J Nucl Med* 20:794-795, 1979
17. Prando A, deSantos LA, Wallace S, et al: Angiography in giant cell bone tumors. *Radiology* 130:323-331, 1979
18. Laurin S: Angiography in giant cell tumor. *Radiology* 17:118-123, 1977
19. Lundstrom B, Lorentzon R, Larson SE, et al: Angiography in giant cell tumors of bone. *Acta Radiol* 18:541-553, 1977
20. Genant HK, Kozin F, Bekerman C: The reflex sympathetic dystrophy syndrome. *Radiology* 117:21-32, 1975
21. Allman RM, Brower AC: Circulatory patterns of deossification. *Radiol Clin of North Am* 19:553-570, 1981
22. Rosenthal L: Role of radionuclide imaging in benign bone and joint diseases with orthopedic interest. In *Nuclear Medicine Annual 1980*, Freeman LM, Weissman HS, eds. New York, Raven Press, 1980, 267-302
23. McNeil BJ, Cassady JR, Geiser CF, et al: Fluorine-18 bone scintigraphy in children with osteosarcoma or Ewing's sarcoma. *Radiology* 109:627-631, 1973
24. Jones SE, Salmon SE: The role of radionuclides in clinical oncology. *Semin Nucl Med* 6:331-346, 1976
25. Makhija MC: Bone scanning in aneurysmal bone cyst. *Clin Nucl Med* 6:500, 1981
26. Lutzker LG, Alavi A: Bone and marrow imaging in sickle cell disease: Diagnosis of infarction. *Semin Nucl Med* 6:83-94, 1978
27. Gelfand MJ, Harcke HT: Skeletal imaging in sickle cell disease. *J Nucl Med* 19:698, 1978
28. Averill RM, Smith RJ, Campbell CJ: Giant cell tumors of the bones of the hand. *J Hand Surg* 5:39-50, 1980
29. Chew FS, Hudson TM: Radionuclide bone scanning of osteosarcoma: Falsely extended uptake patterns. *Am J Roentgenol* 139:49-54, 1982